Photoelectrolysis of clopyralid wastes with a novel laser-prepared MMO-RuO_2TiO_2 anode

Géssica O. S. Santos[a,b,c], Katlin I. B. Eguiluz[a,b], Giancarlo R. Salazar-Banda[a,b], Cristina Saez[c], Manuel A. Rodrigo[c,*]

[a] *Electrochemistry and Nanotechnology Laboratory (LEN), Research and Technology Institute (ITP), Aracaju, SE, Brazil*

[b] *Processes Engineering Post-graduation - PEP, Universidade Tiradentes, 49037-580 Aracaju, SE, Brazil*

[c] *Department of Chemical Engineering, Universidad de Castilla-La Mancha, Campus Universitario s/n, 13071 Ciudad Real, Spain*

Abstract: This paper studies the applicability of a novel laser-prepared mixed metal oxide (MMO-RuO_2TiO_2) anode in the photoelectrochemical degradation of clopyralid, a toxic and biorefractory herbicide. Results are compared to those obtained using the well-known boron-doped diamond (BDD) anode and demonstrate that, although the electrolysis with diamond is more effective than that obtained with the new electrode, the irradiation of UVC light makes the novel MMO material more effective in chloride media. It was explained in terms of the homolysis of hypochlorous acid/ hypochlorite to form chloride and hydroxyl radicals. Photoelectrochemical degradation with MMO produced a marked synergistic effect in TOC removal, especially in the presence of chloride ions. On the contrary, for the BDD anode, at the tested conditions, antagonisms were found in both sulfate and chloride media. These important synergisms allows finding conditions in which the novel anode can be competitive with the BDD.

Keywords: Laser; MMO; BDD; electrolysis; photoelectrolysis

Highlights

- Photoelectrolysis with a novel laser-prepared MMO-RuO_2TiO_2 shows superb performance
- Activation of hydroxyl and chlorine radicals explains the better photoelectrolysis performance
- Under no activation of chlorine radicals, better behavior of BDD
- Photolysis is inefficient in clopyralid removal but alters electrolysis performances

*Author to whom all correspondence should be addressed: manuel.rodrigo@uclm.es

1. Introduction

The contamination of water with pesticides, often associated with intense agriculture activities, is a highly significant environmental issue (Rodrigo et al., 2014; Almazán-Sánchez et al., 2017). During recent decades, diverse technologies have been proposed to remove these pollutants from the water (Jiménez et al., 2016; Trellu et al., 2016; Barba et al., 2017). Biological treatments are the cheapest processes (Acosta-Santoyo et al., 2019), but the high toxicity and poor biodegradability of these molecules make them inefficient in many cases. Because of that, the evaluation of efficient technologies capable of removing complex pollutants from water is not only a topic of significant interest nowadays, but for sure it will be a relevant topic of significant research in the near future (Radjenovic and Sedlak, 2015; Dos Santos et al., 2017; Morillo and Villaverde, 2017).

Oxidation technologies based on the generation and use of hydroxyl radical as an oxidant, namely advanced oxidation processes (AOPs), have attracted significant attention, because of their ability to oxidize recalcitrant organics(Sirés et al., 2014; Martinez-Huitle et al., 2015). Within them, AOPs based on electrochemical oxidation, the so-called electrochemical advanced oxidation process (EAOP), stands out due to the high efficiencies reached in the removal of pollutants, explained in terms of the combination of direct (by electron transfer) and mediated (through the action of oxidants electrogenerated) oxidation mechanisms (Sirés et al., 2014; Moreira et al., 2017).

In electrochemical oxidation (EO), the choice of the anode material is of great importance. Among them, boron-doped anodes (BDD) and mixed metal oxides (MMO) are the most studied, because of their significant differences and the important possibilities of use in real applications (Polcaro et al., 2009; Fornazari et al., 2012; Sirés et al., 2014; de Mello et al., 2018). BDD anodes show advantages such as electrochemical stability, wide potential window, good conductivity and capability of electrogeneration of large amounts

of powerful hydroxyl radicals, which make them suitable to treat a wide range of organic pollutants (Scialdone et al., 2009; Mascia et al., 2011; Sopaj et al., 2015; Coledam et al., 2017). On the other hand, research on MMO application for electrochemical oxidation of recalcitrant pollutants has become attractive due to lower cost of these anodes (Wu et al., 2014; da Silva et al., 2018), although their lower efficiency in the oxidation of organics strongly advices their combination with other technologies in order to make more attractive their use.

Thus, synergic effects can be achieved by the combination of EO with other oxidation technologies, such as irradiation with ultraviolet light (UV) (de Vidales et al., 2019). It is well-known that UVC irradiation can activate oxidants in the bulk solution (Brillas and Martínez-Huitle, 2015; Dos Santos et al., 2017), contributing to minimize the typically found mass transfer limitations bottleneck in the electrochemical treatments, observed specially when the organic concentration reaches low values (Cotillas et al., 2016). In parallel, if anode material has photoactivity, electron-hole pairs are generated, promoting the production of •OH at the anode surface.

With this background, this paper aims to investigate the feasibility of photoelectrochemical oxidation (PEC) using a laser-prepared MMO-RuO_2TiO_2 and to compare results with those obtained using a commercial BDD anode, which is the anode with the best performance known. Then, the oxidation of the herbicide clopyralid has been used as a test reaction, and the PEC process was compared with single photolysis or single electrochemical oxidation (EO), trying to determine if the combination of technologies lead to synergistic effects.

2. Methodology

2.1 Chemicals

Clopyralid purchased from Sigma Aldrich was of analytical grade (99%). Sodium chloride and anhydrous sodium sulfate used as supporting electrolytes purchased from Panreac. Methanol and formic acid used for the mobile phase of HPLC were purchased from Sigma-Aldrich. All aqueous solutions were prepared using high-purity water (Millipore Milli-Q system, resistivity > 18 MΩ). All reactants were of analytical grade and were used as received.

2.2 Physical characterization

The surface morphology of the BDD films was visualized employing a field emission scanning electron microscope (FE-SEM; Zeiss GeminiSEM 500). The elemental chemical composition of the laser prepared MMO-Ti/RuO_2TiO_2 was determined using energy-dispersive X-ray (EDX) spectroscopy coupled to the SEM equipment. X-ray diffraction pattern (XRD) measurements were carried out by using a Bruker-D8 Advance X-ray diffractometer with Cu Kα radiation over a 2θ range between 20° and 80°, at a scan rate of 0.02° min^{-1}.

2.3 Electrochemical characterization

The electrochemical measurements were performed on an Autolab PGSTAT302N (Metrohm – Pensalab) using a conventional three-electrode cell. The counter electrode was a platinum wire, an Ag/AgCl reference electrode, and a 4 cm^2 working electrode, which consisted of laser prepared MMO-Ti/RuO_2TiO_2 and a commercial BDD. Cyclic voltammetry measurements were performed at the potential limits of 0.0–1.2 V for MMO and 0.0–3.0V for BDD anode with a scan rate of 20 mV s^{-1} in Na_2SO_4 (3.0 g L^{-1}) and NaCl solution at the same ionic strength (≈ 0.06).

2.4 Experimental set-up

The electrochemical oxidation, photolysis, and photoelectrochemical oxidation were carried out in a single compartment electrochemical cell. The electrode gap between both electrodes was 1.0 cm, and the capacity of the cell was 150 mL. The applied current density was fixed at 30 mA cm^{-2} provided by potentiostat / galvanostat 302N. For the photolysis, a UVC lamp (with 254 mm) was used to irradiate 7, 9, and 11 W directly to the solution.

2.5 Analytical techniques

Inorganic ions (Cl^-, ClO^-, ClO_3^-, ClO_4^-) were measured using ion chromatography. The hypochlorite measurement was carried by titration because of the interference of this peak with that of chloride. A solution of As_2O_3 in 2.0 M in 2.0 M NaOH (0.001 M) was used to determine the hypochlorite concentration. The total organic carbon (TOC) concentration was monitored using a TOC analyzer Multi N/C 3100 Analytik Jena. The concentration of the clopyralid was quantified by HPLC (Agilent 1100 series), equipped with an Eclipse Plus C-18 column (4.6mm x 100mm; 3.5μm). The mobile phase was a mixture of 30% methanol and 70% formic acid (0.1%) at a flow rate of 1 mL min^{-1}, with the detection achieved at 280 nm. The injection volume was 20.0 μL, the column temperature was set to 20 ºC, and the retention time was around 2.7 min. Acids were identified by an HPLC equipped with a Zorbax SB-Aq, column (4.6mm x 150mm), the mobile phase consists of 4 mM H_2SO_4 with detection at 210 nm. The intermediates were identified by the retention time comparison with standard solutions.

2.7 Synergy coefficient

The synergy coefficient (%) is used to evaluate the effect of the coupling of different processes. For the photo-electrochemical oxidation process, it can be calculated according to Eq. (1) where *k* is the kinetic constant calculated for the different studied processes (electrochemical oxidation, photolysis, and photo-electrochemical oxidation) (Cotillas et al., 2016).

$$\text{Synergy coefficient (\%)} = \frac{k\text{photoelectro} - k\text{photo} - k\text{electro}}{k\text{photo} + k\text{electro}} \times 100 \quad (1)$$

3. Results and discussion

3.1 MMO-Ti/TiO_2RuO_2 characterization

Fig. 1a shows a SEM image of the MMO-Ti/TiO_2RuO_2 used in this study and fabricated by a new CO_2 laser process (Santos et al., 2019). As seen, the more important advantage of this novel electrode is that the morphology of Ti/TiO_2RuO_2 does not present the typical "cracked-mud" surface for metal-oxides coatings on titanium substrates (Wu et al., 2012; De Moura et al., 2014), being this improvement attributed to the novel preparation method employing laser as the heating source (Santos et al., 2019). As reported, the use of a laser allows rapid heating and almost instant cooling, leading to an improved anode surface, which attains longer lifetimes and enhanced performance. The elemental composition analysis (**Figs. 1b and 1c**) of the coatings obtained through EDX reveals that RuO_2 and TiO_2 are well distributed onto the anode surface, with proportions very close to those of the initial precursor solution (66.7% of TiO_2 and 33.3% of RuO_2).

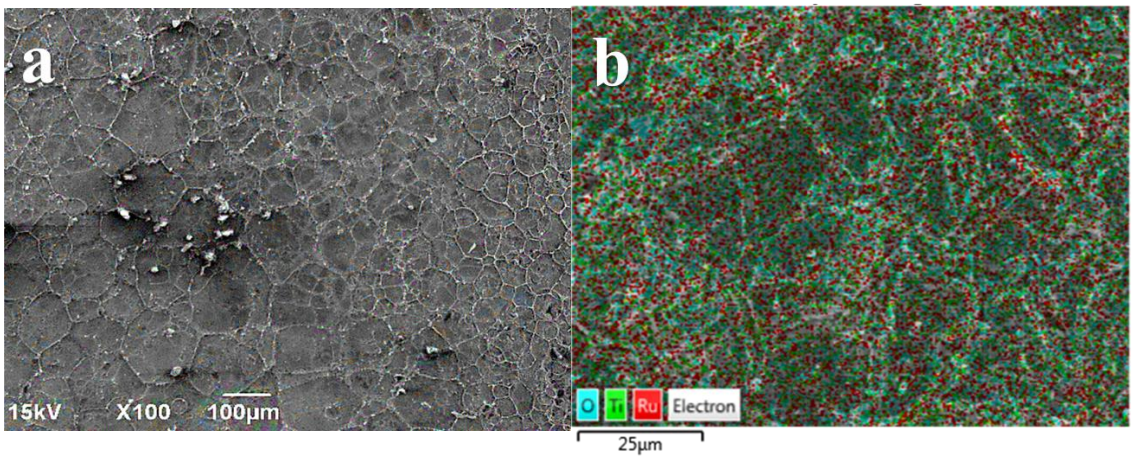

171

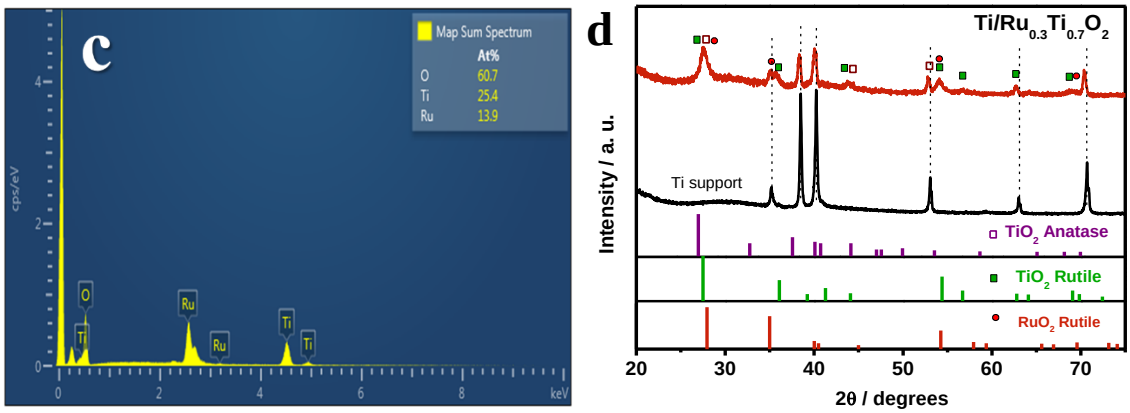

172

173 **Fig. 1.** a) SEM image; b) Elemental mapping image; c) Elemental analysis and d) XRD
174 pattern of the new MMO-RuO_2TiO_2 anode. The XRD pattern of the Ti substrate is also
175 shown in d).

176

177 The crystallinity and crystalline phases of the prepared RuO_2TiO_2 coating were studied
178 by XRD **(Fig. 1d).** According to the Joint Committee on Powder Diffraction Standards
179 (JCPDS), the corresponding main diffraction peaks in the XRD patterns are attributed to
180 the RuO_2 in the rutile phase (JCPDS no. 00-040-1290) and TiO_2 both in rutile (00-004-
181 0551) and anatase (JCPDS 00-00109562). Additionally, the XRD pattern of the metallic
182 Ti support is also observed due to X-ray penetration through the oxides films (de Mello
183 et al., 2018; Santos et al., 2019).

184

Regarding electrochemical characterization, cyclic and linear voltammetry curves of the novel MMO-TiO_2RuO_2 were recorded in Na_2SO_4 (3.0 g L^{-1}) and NaCl (3.7 g L^{-1}) as supporting electrolytes at the same ionic strength (≈ 0.06) **(Fig. 2).** Results for BDD anode are also provided to explain the distinct behavior of each anode. From the cyclic voltammetry curves in both electrolytes **(Figs 2a** and **2c)**, it is clear to note the very distinct behavior of each anode. While the MMO anode presents a typical behavior of this kind of anode with a broad double layer region in the potential interval before oxygen evolution reaction (OER), the BDD anode presents a typical behavior of "non-active anodes" with high O_2 overpotential and low background currents. Moreover, linear sweep voltammetry curves presented in **Figs 2b** and **2d** shows that the OER for the MMO-TiO_2RuO_2 occurs at rather low potentials (1.1 V *vs*. Ag/AgCl) while for the for BDD anode almost no current response until applied potentials over 1.5 V *vs.* Ag/AgCl are seen. This significant difference in the OER potential at the anodes can promote substantial variations on the oxidants' production, which will be investigated hereafter.

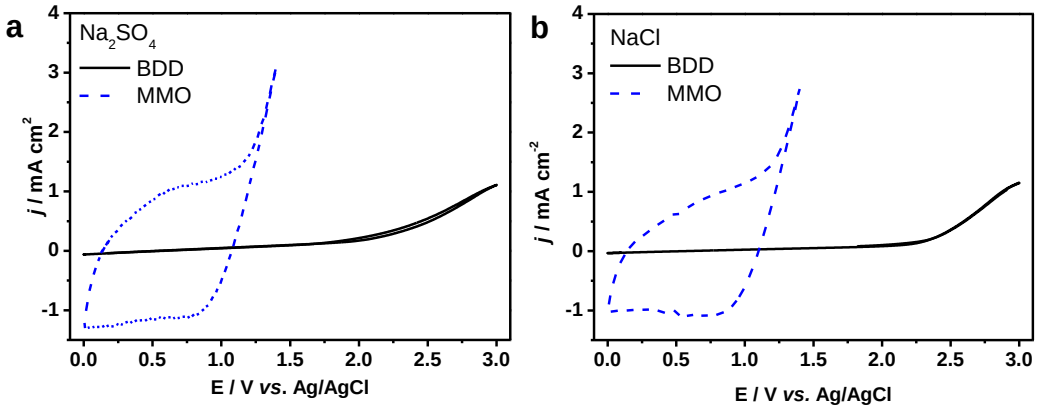

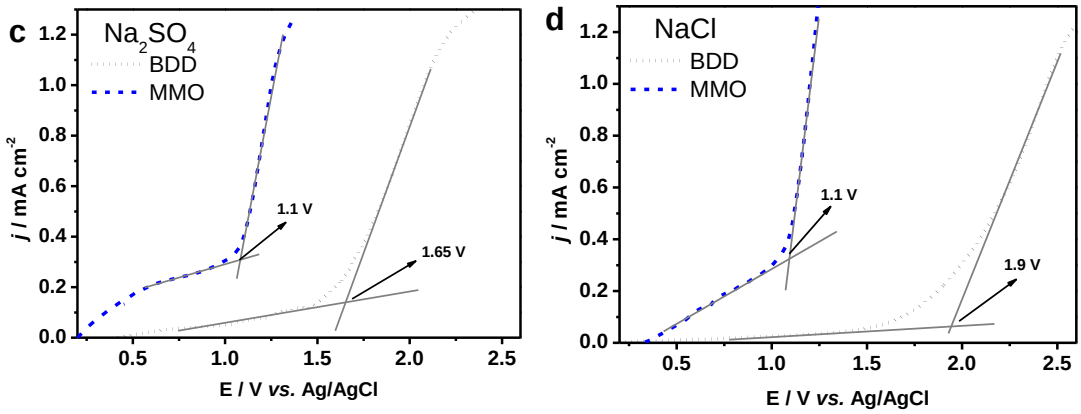

Fig. 2. Cyclic voltammetry curves of Ti/TiO_2-RuO_2 (MMO) and BDD anodes obtained at a scan rate of 20 mV s^{-1} in (a) Na_2SO_4 and (b) NaCl supporting electrolyte and linear sweep voltammetry curves of Ti/TiO_2-RuO_2 (MMO) and BDD obtained at a scan rate of 10 mV s^{-1} in (c) Na_2SO_4 and (d) NaCl supporting electrolyte. Na_2SO_4: 3.0 g L^{-1} and NaCl: 3.7 g L^{-1}.

3.2 Chlorine speciation in electrochemical and photoelectrochemical process

Understanding the role of chloride is important in order to discuss the expected differences produced in the oxidation via photolysis of electrogenerated free chlorine. **Fig. 3** shows the chlorine species electrogenerated in the solution during 8 h of electrochemical and photoelectrochemical oxidation of NaCl 3.0 g L^{-1} with both MMO and BDD anodes (this latter electrode used for the sake of comparison). The important differences observed in the chlorine speciation, for single electrochemical oxidation, can be correlated to the linear sweep voltammograms response of each anode employed **(Fig. 2d).** Considering the MMO-RuO_2TiO_2 shows a low overpotential of 1.1 V *vs*. Ag/AgCl for chlorine evolution reaction, it can explain the higher concentrations of hypochlorite as compared to those obtained with the BDD anode. Chlorine is produced on the anode surface by the reaction shown in Eq. (2), and then, it is disproportionated to hypochlorite/hypochlorous acid, Eqs. (3–4).

$$2Cl^- \rightarrow Cl_2 + 2e^- \quad (2)$$

$$Cl_2 + 2OH^- \rightarrow H_2O + ClO^- + Cl^- \quad (3)$$

$$HClO \leftrightarrow H^+ + ClO^- \quad (4)$$

In contrast, large quantities of hydroxyl radicals are formed at the BDD surface (Eq. (5)) that are in co-existence with the active chlorine species, which means that during electrolysis of aqueous solutions in the presence of chlorides, these radicals can oxidize Cl^- successively to different oxochlorinated compounds (Eqs. (6–9)) (Vacca et al., 2013; Sirés et al., 2014; Do Nascimento Brito et al., 2015).

$$H_2O \rightarrow BDD\ ^{\bullet}OH + H^+ + e^- \quad (5)$$

$$Cl^- + {}^{\bullet}OH \rightarrow ClO^- + H^+ + e^- \quad (6)$$

$$ClO^- + {}^{\bullet}OH \rightarrow ClO_2^- + H^+ + e^- \quad (7)$$

$$ClO_2^- + {}^{\bullet}OH \rightarrow ClO_3^- + H^+ + e^- \quad (8)$$

$$ClO_3^- + {}^{\bullet}OH \rightarrow ClO_4^- + H^+ + e^- \quad (9)$$

Because of that, chlorates measured are much higher (1582 mg L^{-1}) with BDD than with MMO-RuO_2TiO_2 (62.48 mg L^{-1}) and, even, perchlorates (233.35 mg L^{-1}) are formed with BDD while no perchlorate is seen for MMO. The chlorate anions observed with the MMO are most likely formed by a well-known disproportionation process, shown in Eq. (9) (Bolyard et al., 1992), favored in the electrochemical cells and also well-known to be promoted during aging of hypochlorite solutions.

$$3\ ClO^- \rightarrow ClO_3^- + 2\ Cl^- \quad (9)$$

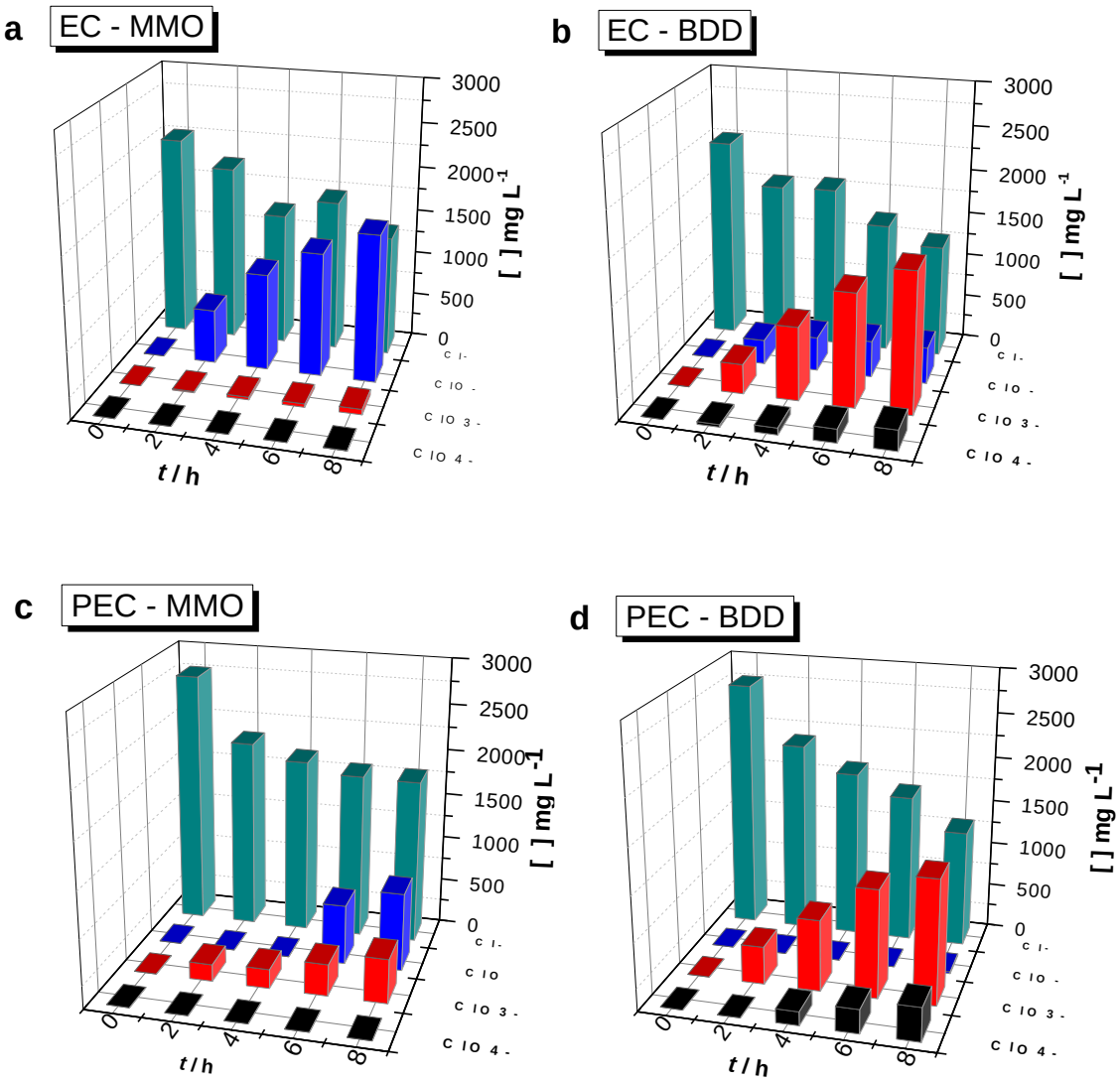

Fig. 3. Evolution of chlorine species as a function of electrochemical oxidation and photoelectrochemical oxidation time for MMO anode (a,c) and BDD anode (b,d): ■ Cl^- ■ ClO^- ■ ClO_3^- ■ ClO_4^- species.

When UVC light irradiates the solution, reduction of the concentration of hypochlorite, for both MMO and BDD, shows that under the conditions at which the test was performed (j = 30 mA cm^{-2} and pH ≈ 3.8), chlorine and hydroxyl radicals can be formed by a homolytic homogeneous reaction (Eq. (10)) of HClO by UVC radiation in the bulk solution.

$$HClO + h\upsilon \rightarrow Cl^{\bullet} + {}^{\bullet}OH \quad (10)$$

Recently, Hurwitz *et al.* (Hurwitz et al., 2014) and Sanchez-Montez *et al.* (Sanchez-Montes et al., 2017) have shown that the photo-assisted method can be successfully employed to promote the homolysis of the *in-situ* electrogenerated active chlorine species using low power UVC lamps in the bulk solution. These radicals are expected to improve oxidation and mineralization of pollutants in the combined process, in comparison to the single electrochemical oxidation or the photolysis (Sanchez-Montes et al., 2017). Speciation of chlorine is essential to be checked since in both, electrochemical oxidation and photoelectrochemical oxidation, the formation of chlorates and perchlorates may occur. As it is known, these species are not efficient in the oxidation of organic compounds.

Moreover, it is essential to point out that the amount of available oxidants is affected by a photoactive anode, where chloride ions might be oxidized at a less positive potential under photoelectrocatalytic conditions, as denoted by Eq. (11) (Do Nascimento Brito et al., 2015; Aquino et al., 2017).

$$TiO_2 - hvb^{+} + Cl^{-} \rightarrow TiO_2 - Cl^{\bullet} \quad (11)$$

For the MMO anode, hypochlorite is reduced by 64% with the irradiation of UCV light. Besides, no perchlorates are formed during the photoelectrochemical oxidation, but the chlorates formation increases 7.74 times (from 62.38 to 483.2 mg L^{-1}). This increase can be explained in terms of the formation of hydroxyl and chlorine radicals during this process by the homolysis of hypochlorous acid/hypochlorite. For the BDD anode,

chlorate and perchlorate formation increase 13% and 37%, respectively, associated with a decrease of 94.8% in the concentration of hypochlorite. Again, the homolysis of hypochlorite to produce hydroxyl and chlorine radicals in bulk may help to explain the results obtained.

3.3 Clopyralid degradation and mineralization

Fig. 4 shows the clopyralid degradation and mineralization during the electrochemical oxidation using MMO-RuO_2TiO_2, at a fixed current density of 30 mA cm^{-2}, in the absence and presence of chloride. Results are compared to those obtained using BDD. It can be observed a very distinct behavior considering electrolyte media and anode material. In Na_2SO_4 electrolyte media **(Fig. 4a)**, the BDD anode was more effective than the MMO, achieving 76% of mineralization after 8 h of treatment, whereas the MMO was able to remove only 7% of clopyralid accompanied by only a 4% of mineralization. The results for MMO in sulfate media are in agreement with previous results shown in the literature, which indicate that MMO anodes produce $^{\bullet}OH$ chemisorbed on its surfaces, which is non-very effective to oxidize organic matter and to electrogenerate other powerful oxidants.

On the other hand, as it has been well stated during the last two decades when BDD is employed in sulfate media, sulfate is known to be transformed into peroxosulfate by the action of physisorbed $^{\bullet}OH$. This oxidant is then, expected to react with other oxidants and extend the oxidation reactions to the bulk of the wastewater promoting the formation of $^{\bullet}OH$ and $(SO_4^{-})^{\bullet}$, which are very effective in the oxidation of organics.

Furthermore, the efficient production of these hydroxyl radicals is a crucial factor in explaining the results of the electrochemical oxidation, and, for this reason, it is accepted that the oxidation ability of the electrochemical oxidation depends on the anode used and

the efficient production of hydroxyl radicals on its surface (Wu et al., 2012; De Moura et al., 2014).

However, when Cl^- ions are present, the hypochlorite/hypochlorous acid is the primary expected mediator. Thus, significant differences are expected, considering both anodes. For BDD anode, a reduction of clopyralid removal from 76.0% in sulfate media to 47.6% in chloride media is observed. It can be explained considering the scavenger effect due to large amount of hydroxyl radicals onto the BDD surface reacting to generate chlorine species. These species form rapidly chlorates and perchlorates, which are kinetically less efficient in the oxidation of clopyralid than hypochlorite/hypochlorous acid.

For MMO, when chloride is contained in the waste, a significant improvement in the clopyralid removal is observed (from 7.0% to 51.2%), although TOC was maintained. These results confirm the indirect oxidation is occurring in the bulk solution due to the high amount of hypochlorite electrogenerated and the •OH generated by homolysis, favoring accumulation of intermediates.

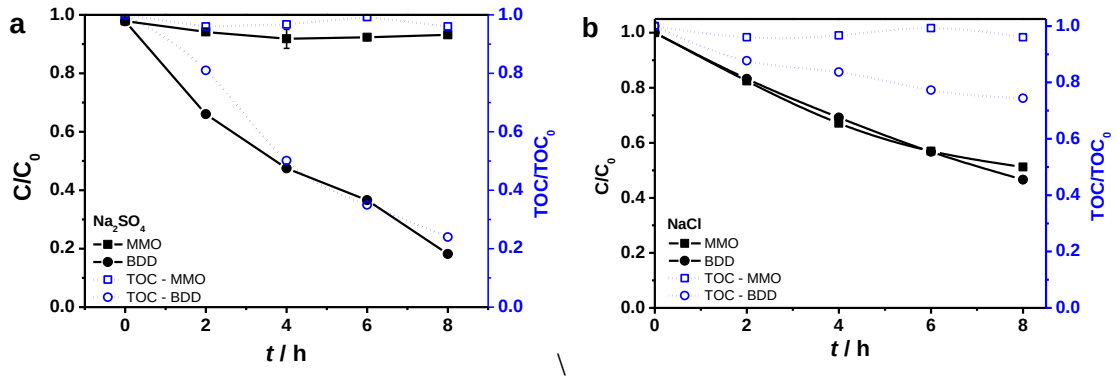

Fig. 4: Clopyralid (solid symbols) and TOC (open symbols) removal with time during electrochemical oxidation with BDD (●,○) and MMO (■,□) in Na_2SO_4 3 g L^{-1} (a) and NaCl 3.7 g L^{-1} (b). C_0: 100 mg L^{-1}; *j*: 30 mA cm^{-2}; V: 150 mL; cathode: Pt.

In search of better efficiencies, a combination of electrochemical oxidation with UVC irradiation (photoelectrochemical oxidation) was evaluated. However, before coupling UV light with electrochemical oxidation, the evaluation of single photolysis using UVC lamps of 7, 9, and 11 W was also performed in order to evaluate the effect of the power on the efficiency of single photolysis. For the three lamps, no significant changes in TOC removal were observed (values even higher than the initial because of the soft transformation of the clopyralid into other compounds which may have a different response in the TOC analyzer) (**Fig. S1**). Among the lamps, 9 W presented the best outcomes with a transformation of 8.3% and 14.1% of clopyralid in sulfate and chloride media, respectively, and for this reason, it was chosen as UVC source of irradiation for the photoelectrochemical process.

As previously seen, single photolysis is not a suitable technology to be used for this kind of compound, but in the coupled process, considerable differences are expected. Both sulfate and chloride species can be activated differently by the UVC light in different anodes. **Fig. 5** shows the removals of clopyralid and TOC as a function of time in sulfate and chloride media during photoelectrochemical oxidation using a 9 W UVC lamp with both anodes. In sulfate media, the efficiency of BDD anode drastically reduces from 76.0 % to 52.41%. This reduction can be attributed to the self-scavenging effect, where $^{\bullet}OH$ begins to react to deactivate the strong oxidant species formed. Also, more recalcitrant compounds may be favored by light, since only 24% of TOC removal is attained by photoelectrolysis, while 76% was reached without irradiation in the same reaction time (8.0 h). For chloride media, an impressive improvement was observed, resulting in 99.1% of clopyralid removal, which can result mainly from the contribution of mediated oxidation in bulk, as previously demonstrated. However, TOC removal improvement is much less significant (55.7%), which can be associated with formation of more

recalcitrant by-products, more challenging to attack than those observed for single electrochemical oxidation with BDD.

On the other hand, the combination of the electrochemical process with MMO as anode with the irradiation of 9 W UVC synergistically enhances clopyralid removal from 7% to 19% in Na_2SO_4 media and from 51.2 to 58.4% in NaCl media. TOC removal increases, more importantly, being more significant for NaCl media, presenting a 53.6% removal after photoelectrochemical oxidation, which is much higher than that for single electrochemical oxidation (4.0%) and comparable to the value reached by the BDD anode, which becomes an outstanding result.

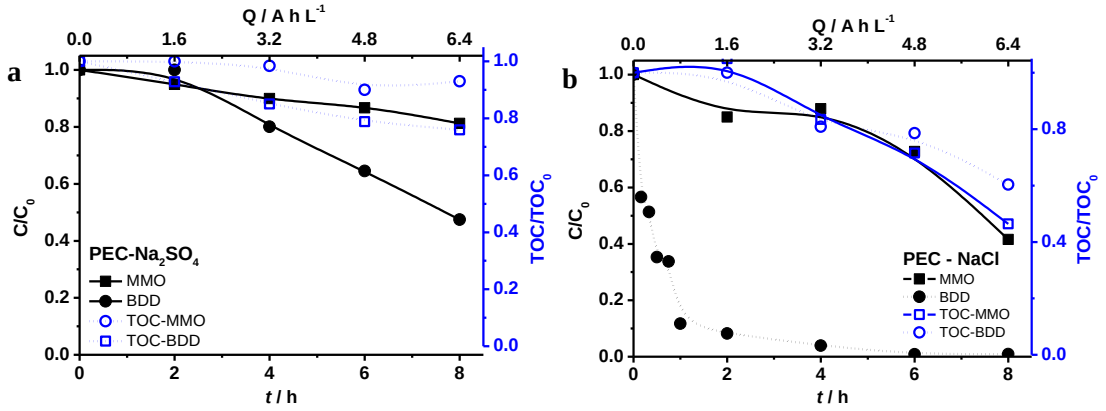

Fig. 5. Clopyralid (solid symbols) and TOC (open symbols) removal with time during photoelectrochemical oxidation with BDD (●,○) and MMO (■,□) in Na_2SO_4 3 g L^{-1} (a) and NaCl 3.7 g L^{-1} (b). C_0: 100 mg L^{-1}; *j*: 30 mA cm^{-2}; V: 150 mL; cathode: Pt.

Hurwitz *et al*. compared BDD and DSA-Cl_2 and found that due to its enhanced anodic properties, BDD was much more effective than DSA-Cl_2 at direct anodic oxidation in the absence of chloride, but was less effective with chloride present due to lower free chlorine production. Those results are in agreement with the results found in this work, but the new anode material demonstrates outstanding properties when combined with UVC irradiation and here, it is demonstrated that the new MMO anode tested can be

competitive with BDD in the treatment of wastes containing chlorides when combined with UCV irradiation.

Regarding intermediates, they were monitored by HPLC. Picolinic acid and 6-chloropicolinic were identified as the main produced oxidation by-products **(Figs. S2 and S3)** during clopyralid degradation using electrochemical oxidation. Photoelectrochemical oxidation showed, in addition to the production of these intermediates, other non-identified species but at rather low concentrations. As the final stage of the mineralization reaction, the observed residual organic load is due to the generated short-chain carboxylic acids **(Fig. S4),** mainly as oxalic, oxamic and maleic acid.

3.3 Kinetics study

Kinetic study of both clopyralid and TOC removal revealed a pseudo-first-order kinetic model (Eq. (12)) that could be well-fitted with the experimental data for the different studied processes (electrochemical oxidation, photolysis, and photo-electrochemical oxidation) (de Vidales et al., 2019).

$$\ln \frac{C_0}{C} = k \cdot t \qquad (12)$$

The rate constants for the clopyralid removal (k_{clop}) and mineralization (k_{TOC}) when using distinct processes and UVC lamps are summarized in **Table 1**. As observed, the values of mineralization kinetic constants calculated for single photolysis were null due to the absence of TOC removal. Also, values calculated for the removal of clopyralid were shallow, pointing out the low efficiency of the photolytic process. For the photoelectrochemical oxidation, kinetic rates were higher than single electrochemical oxidation in all cases employing the MMO anode. On the contrary, in chloride media,

only clopyralid removal kinetic rate was improved by coupling UVC with electrochemical oxidation with BDD anodes, while a decrease in the kinetic rate for both clopyralid and TOC removal is observed for photoelectrochemical process with BDD in sulfate media. For chloride media, the TOC removal also slightly improved.

Table 1. Observed kinetic constants for clopyralid and TOC removal by the different process after 8 h in 3.0 g L^{-1} of Na_2SO_4 and 3.7 g L^{-1} of NaCl.

Anode	Media	Process	% Clopyralid removal	k_{clop} / min^{-1}	% TOC removal	k_{TOC} / min^{-1}
MMO	SO_4^{-}	EC	7 ± 0.1	0.0059	4	0.00103
BDD		EC	81.8	0.202	76 ± 0.02	0.1740
MMO		PEC 9 W	18.76	0.02533	6.95	0.01245
BDD		PEC 9 W	52.41	0.03560	24.06	0.09636
–		PC 7 W	2.23	0.000515	9.5	–
		PC 9 W	8.25	0.01029	0	–
		PC 11 W	7.61	0.00948	5.74	–
MMO	Cl^{-}	EC	51.22	0.0914	3.97	0.00641
BDD		EC	47.6	0.0955	25.61	0.03595
MMO		PEC 9 W	58.4	0.09551	53.6	0.05250
BDD		PEC 9 W	99.1	1.23007	39.7	0.06258
–		PC 7 W	4.05	0.000064	0	–
		PC 9 W	14.08	0.02118	0	–
		PC 11 W	7.25	0.00947	5.72	–

To better observe the influence of UVC irradiation on the performance of the electrolysis, **Fig. 6** shows the effect of the anode material and the supporting electrolyte on the synergy coefficient when coupling electrochemical oxidation with UVC light. Here, we found antagonistic effects in both clopyralid and TOC removal in sulfate media at BDD anode (–83.2% and –44.6%). On the contrary, when using the MMO anode in sulfate media

coupled with UVC light, a very high synergistic effect was found for clopyralid and TOC removal (56.5% and 87.08%). It indicates a clear contribution of photolysis for molecule breakage into intermediates, which are more easily attacked by the photo-activated persulfate allowing to more significant removals for MMO when compared to single electrochemical oxidation.

When coupling technologies in chloride media, for BDD anode, we found the maximum synergy coefficient (954.2%) for the clopyralid removal which is attributed to occurrence of another mechanism related to rapid chlorination of molecule from mediated oxidation of chlorine species activated by light. However, it is essential to remark that mineralization is not attained, even an antagonistic value of –74.07 for TOC removal suggest formation of more recalcitrant species. Finally, the coupled process in chloride media shows an almost null synergy effect for clopyralid removal with MMO anode, but surprisingly, a marked synergistic effect for TOC removal occurs (719.09 %), although not meaning complete removal of organic matter. This fact again points out the very significant contribution of photolysis and activated chlorine on the clopyralid degradation.

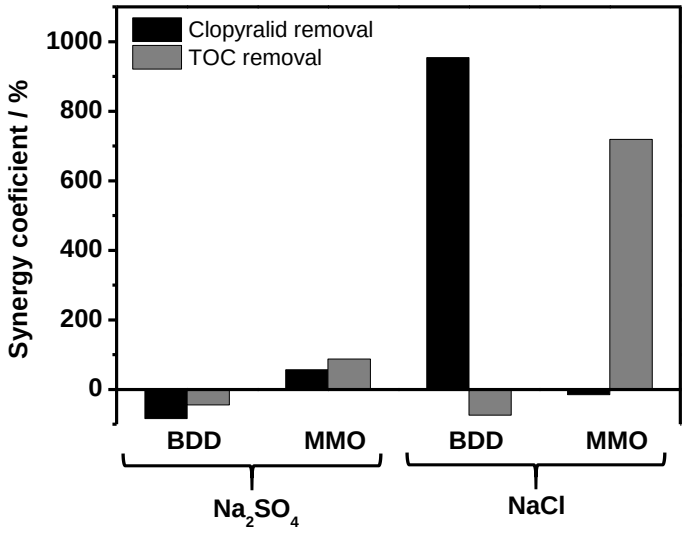

Fig. 6. Effect of anode material and supporting electrolyte on the observed synergism/antagonism of UVC 9 W in terms of clopyralid removal and mineralization; ■ Clopyralid removal; ■ TOC removal.

4. Conclusions

From this work, the following conclusions can be drawn:

- Important differences in the degradation of clopyralid wastes using electrolysis, photolysis, and photoelectrolysis were observed. Photolysis is not efficient alone, but it strongly modifies the performance of electrolysis, both in sulfate and chloride supporting electrolytes, because of the activation of the oxidants electrogenerated.
- Removal efficiencies depend on both the electrode and the electrolyte used. The significant differences in the OER overpotential at both anodes promote a substantial variation on the oxidants production, and this fact helps to explain the different results observed.
- The formation of hydroxyl radicals explains the formation of chlorate and perchlorate during the electrolysis with diamond. The substantial increase in the production of chlorates during the photoelectrolysis is a clear indicator of the formation of hydroxyl radicals by the homolysis of chlorine oxidative species.
- Light irradiation does not improve but deteriorates the performance of the electrolysis in sulfate media.
- The novel laser-prepared MMO-RuO_2TiO_2 shows outstanding performance during the photoelectrolysis of clopyralid wastes, being more effective than diamond anode in chloride media.

- Homolysis of chlorine oxidation species to chlorine and hydroxyl radicals can help to explain the better behavior observed during the photoelectrolysis with the new laser-prepared MMO-RuO_2TiO_2

Acknowledgments

Financial support from the Agencia Estatal de Investigación through projects CTQ2017-91190-EXP and CTM2016-76197-R (AEI/FEDER, UE) is gratefully acknowledged. The authors also acknowledge the financial support from the Brazilian agencies CNPq (305438/2018-2 and 310282/2013-6), CAPES (88882.365552/2018-01 and 88881.187890/2018-01) and FAPITEC/SE. We would also like to thank Prof. Dr. Ronaldo Santos from the Federal University of Sergipe for the equipment for the CO_2 laser synthesis.

References

Acosta-Santoyo, G., Solís, S., Hernández-Silva, G., Cárdenas, J., Plank, Z., Bustos, E., 2019. Analysis of the biological recovery of soils contaminated with hydrocarbons using an electrokinetic treatment. J. Hazard. Mater. 371, 625-633.

Almazán-Sánchez, P.T., Cotillas, S., Sáez, C., Solache-Ríos, M.J., Martínez-Miranda, V., Cañizares, P., Linares-Hernández, I., Rodrigo, M.A., 2017. Removal of pendimethalin from soil washing effluents using electrolytic and electro-irradiated technologies based on diamond anodes. Appl. Catal. B 213, 190-197.

Aquino, J.M., Miwa, D.W., Rodrigo, M.A., Motheo, A.J., 2017. Treatment of actual effluents produced in the manufacturing of atrazine by a photo-electrolytic process. Chemosphere 172, 185-192.

Barba, S., Villaseñor, J., Rodrigo, M.A., Cañizares, P., 2017. Effect of the polarity reversal frequency in the electrokinetic-biological remediation of oxyfluorfen polluted soil. Chemosphere 177, 120-127.

Bolyard, M., Fair, P.S., Hautman, D.P., 1992. Occurrence of chlorate in hypochlorite solutions used for drinking water disinfection. Environ. Sci. Technol. 26, 1663-1665.

Brillas, E., Martínez-Huitle, C.A., 2015. Decontamination of wastewaters containing synthetic organic dyes by electrochemical methods. An updated review. Appl. Catal. B 166, 603-643.

Coledam, D.A., Pupo, M.M., Silva, B.F., Silva, A.J., Eguiluz, K.I., Salazar-Banda, G.R., Aquino, J.M., 2017. Electrochemical mineralization of cephalexin using a conductive diamond anode: A mechanistic and toxicity investigation. Chemosphere 168, 638-647.

Cotillas, S., de Vidales, M.J.M., Llanos, J., Sáez, C., Cañizares, P., Rodrigo, M.A., 2016. Electrolytic and electro-irradiated processes with diamond anodes for the oxidation of

persistent pollutants and disinfection of urban treated wastewater. J. Hazard. Mater. 319, 93-101.
Da Silva, L.M., Santos, G.O.S., de Salles Pupo, M.M., Eguiluz, K.I.B., Salazar-Banda, G.R., 2018. Influence of heating rate on the physical and electrochemical properties of mixed metal oxides anodes synthesized by thermal decomposition method applying an ionic liquid. J. Electroanal Chem. 813, 127-133.
de Mello, R., Santos, L.H., Pupo, M.M., Eguiluz, K.I., Salazar-Banda, G.R., Motheo, A.J., 2018. Alachlor removal performance of $Ti/Ru_{0.3}Ti_{0.7}O_2$ anodes prepared from ionic liquid solution. J Solid State Electr. 22, 1571-1580.
De Moura, D.C., De Araújo, C.K.C., Zanta, C.L., Salazar, R., Martínez-Huitle, C.A., 2014. Active chlorine species electrogenerated on $Ti/Ru_{0.3}Ti_{0.7}O_2$ surface: electrochemical behavior, concentration determination and their application. J. Electroanal Chem. 731, 145-152.
de Vidales, M.J.M., Castro, M.P., Saez, C., Cañizares, P., Rodrigo, M.A., 2019. Radiation-assisted electrochemical processes in semi-pilot scale for the removal of clopyralid from soil washing wastes. Sep. Purif. Technol. 208, 100-109.
Do Nascimento Brito, C., De Araújo, D.M., Martínez-Huitle, C.A., Rodrigo, M.A., 2015. Understanding active chlorine species production using boron doped diamond films with lower and higher sp^3/sp^2 ratio. Electrochem. commun. 55, 34-38.
Dos Santos, E., Sáez, C., Cañizares, P., Martínez-Huitle, C., Rodrigo, M., 2017. UV assisted electrochemical technologies for the removal of oxyfluorfen from soil washing wastes. Chem. Eng. J. 318, 2-9.
Fornazari, A.L.T., Malpass, G.R., Miwa, D.W., Motheo, A.J., 2012. Application of electrochemical degradation of wastewater composed of mixtures of phenol–formaldehyde. Water Air Soil Pollut. 223, 4895-4904.
Hurwitz, G., Pornwongthong, P., Mahendra, S., Hoek, E.M., 2014. Degradation of phenol by synergistic chlorine-enhanced photo-assisted electrochemical oxidation. Chem. Eng. J. 240, 235-243.
Jiménez, C., Sáez, C., Cañizares, P., Rodrigo, M., 2016. Optimization of a combined electrocoagulation-electroflotation reactor. Environ. Sci. Pollut. Res. 23, 9700-9711.
Martinez-Huitle, C.A., Rodrigo, M.A., Sires, I., Scialdone, O., 2015. Single and coupled electrochemical processes and reactors for the abatement of organic water pollutants: a critical review. Chem. Rev. 115, 13362-13407.
Mascia, M., Vacca, A., Polcaro, A.M., Palmas, S., Pozzo, A.D., 2011. Electrochemical treatment of simulated ground water containing MTBE and BTEX with BDD anodes. J. Chem. Technol. Biotechnol 86, 128-137.
Moreira, F.C., Boaventura, R.A., Brillas, E., Vilar, V.J., 2017. Electrochemical advanced oxidation processes: a review on their application to synthetic and real wastewaters. Appl. Cat. B 202, 217-261.
Morillo, E., Villaverde, J., 2017. Advanced technologies for the remediation of pesticide-contaminated soils. Sci. Total Environ. 586, 576-597.
Polcaro, A., Vacca, A., Mascia, M., Palmas, S., Ruiz, J.R., 2009. Electrochemical treatment of waters with BDD anodes: kinetics of the reactions involving chlorides. J. Appl. Electrochem. 39, 2083.
Radjenovic, J., Sedlak, D.L., 2015. Challenges and opportunities for electrochemical processes as next-generation technologies for the treatment of contaminated water. Environ. Sci. Technol. 49, 11292-11302.
Rodrigo, M., Oturan, N., Oturan, M.A., 2014. Electrochemically assisted remediation of pesticides in soils and water: a review. Chem. Rev. 114, 8720-8745.

Sanchez-Montes, I.J., Silva, B.F., Aquino, J.M., 2017. On the performance of a hybrid process to mineralize the herbicide tebuthiuron using a DSA® anode and UVC light: a mechanistic study. Appl. Catal. B 200, 237-245.
Santos, G., Silva, L., Alves, Y., Silva, R., Eguiluz, K., Salazar-Banda, G., 2019. Enhanced stability and electrocatalytic properties of $Ti/Ru_xIr_{1-x}O_2$ anodes produced by a new laser process. Chem. Eng. J. 355, 439-447.
Scialdone, O., Randazzo, S., Galia, A., Silvestri, G., 2009. Electrochemical oxidation of organics in water: role of operative parameters in the absence and in the presence of NaCl. Water Res. 43, 2260-2272.
Sirés, I., Brillas, E., Oturan, M.A., Rodrigo, M.A., Panizza, M., 2014. Electrochemical advanced oxidation processes: today and tomorrow. A review. Environ. Sci. Pollut. Res. 21, 8336-8367.
Sopaj, F., Rodrigo, M.A., Oturan, N., Podvorica, F.I., Pinson, J., Oturan, M.A., 2015. Influence of the anode materials on the electrochemical oxidation efficiency. Application to oxidative degradation of the pharmaceutical amoxicillin. Chem. Eng. J. 262, 286-294.
Trellu, C., Mousset, E., Pechaud, Y., Huguenot, D., Van Hullebusch, E.D., Esposito, G., Oturan, M.A., 2016. Removal of hydrophobic organic pollutants from soil washing/flushing solutions: a critical review. J. Hazard. Mater 306, 149-174.
Vacca, A., Mascia, M., Palmas, S., Mais, L., Rizzardini, S., 2013. On the formation of bromate and chlorate ions during electrolysis with boron doped diamond anode for seawater treatment. J. Chem. Technol. Biotechnol 88, 2244-2251.
Wu, J., Zhang, H., Oturan, N., Wang, Y., Chen, L., Oturan, M.A., 2012. Application of response surface methodology to the removal of the antibiotic tetracycline by electrochemical process using carbon-felt cathode and DSA ($Ti/RuO_2–IrO_2$) anode. Chemosphere 87, 614-620.
Wu, W., Huang, Z.-H., Lim, T.-T., 2014. Recent development of mixed metal oxide anodes for electrochemical oxidation of organic pollutants in water. Appl. Catal. A 480, 58-78.